Synthesis of Gram Quantities of C_{60} by Plasma Discharge in a Modified Round-Bottomed Flask. Key Parameters for Yield Optimization and Purification

Walter A. Scrivens and James M. Tour*

Department of Chemistry and Biochemistry, University of South Carolina, Columbia, South Carolina 29208

Received September 11, 1992

Described is the fabrication of a plasma discharge reactor constructed from a 1-L round-bottomed flask that allows for the preparation of gram quantities of C_{60} in an 8-h period. The modified reactor design (1) is inexpensive, (2) requires almost no machining, (3) has high thru-put, (4) affords high yields of fullerenes, (5) allows one to have near-continuous feed of graphite rods, and (6) permits control over four major reaction parameters important for the clean formation of fullerenes. The four major reaction parameters necessary to control for the high yield of fullerenes are the absolute pressure, the rate of helium gas flow through the reactor, the current level of the arc as determined by the setting on the arc welding unit, and the arc gap maintained by monitoring the current on a clip-on digital AC current meter. Since the apparatus described can allow for easy adjustment of all four major reaction parameters, this design could also be used to study the changes in fulleroid content based on parameter modification. Also detailed is the efficacy of a procedure for the purification of the crude fullerene mixtures using activated charcoal as a chromatographic stationary phase.

Since the initial discovery of buckminsterfullerene (C_{60}) in 1985[1] and the subsequent development of the carbon arc method for producing macroscopic quantities of this material,[2] a large amount of effort has been directed toward the understanding and utilization of this new allotrope of carbon.[3] We describe here the fabrication of a plasma discharge reactor constructed from a 1-L round-bottomed flask that allows for the preparation of gram quantities of C_{60} in an 8-h period. The reactor design (1) is inexpensive, (2) requires almost no machining, (3) allows high thru-put, (4) affords high yields of fullerenes, (5) allows one to have near continuous feed of graphite rods, and (6) permits control over four major reaction parameters important to the clean formation of fullerenes. Since the apparatus described can allow for easy adjustment of all four major reaction parameters, this design could also be used to study the changes in fulleroid content based on parameter modification. We also detail the efficacy of a procedure for the purification of the crude fullerene mixtures using activated charcoal as a charomatographic stationary phase.

The most common method of producing C_{60} utilizes the Huffman-Krätschmer carbon arc method in which graphite electrodes are vaporized in a low pressure helium atmosphere by passing an electrical current through the electrodes, thus generating an arc. The soot produced by this carbon arc contains C_{60} as well as some other higher molecular weight fullerenes. A number of reports on this method have appeared that provide details of the apparati used.[4,5] There are two major variants of the carbon arc method, namely, contact arc and plasma discharge. In the contact arc method, the graphite electrodes are kept in constant contact through either a gravity feed mechanism[4b] or through the use of a feed spring.[4c,e] To date, the most easily accessible apparatus for the contact arc method is the gravity feed apparatus developed by Wudl.[4b] This is a relatively inexpensive and simple device which uses an arc welder as the power source. However, like all other contact arc apparati, it suffers from overheating problems due to resistive heating of the graphite electrodes and the apparatus must be disassembled for the insertion of new graphite rods. The plasma discharge method[4a,d] maintains a constant arc gap between the electrodes, thus avoiding much of the resistive heating problems found in the contact arc methods. This method can potentially produce crude fullerenes more efficiently by providing more control over the conditions which form the fullerenes in the reactor. The drawback to the plasma discharge method is that it requires a fairly complex apparatus with special feed mechanisms to align the electrodes and maintain a constant arc gap. And, like most other methods, the apparatus must be disassembled for the insertion of new graphite rods.

Here we describe the simple fabrication and use of a low cost fullerene generator of the plasma discharge type (Figure 1). The reaction vessel is simply a 1-L Pyrex round-bottomed flask that has had an additional 24/40 female joint affixed opposite to the first joint. The Pyrex guide arms (12 mm o.d.) extend from outside the water cooling bucket and are fitted with vacuum take off adapters and tipped with 24/40 male joints that insert into the reactor vessel (the total length of the guide arm including the male joint is 25 cm). The guide arms help to align the 1-cm-diameter copper mounting rods (each copper mounting rod is 35 cm long). One end of the copper mounting rods has a 3/16 in. diameter hole drilled to a 1-cm depth for mounting the graphite electrodes and on the other end has a screw hole tapped so that the rods can be attached to the arc welder with brass screws. The copper mounting rods extend out through the end of the guide arms and through standard 19/22 septa which have

(1) Kroto, H. W.; Heath, J. R.; O'Brien, S. C.; Curl, R. F.; Smalley, R. E. *Nature* **1985**, *318*, 162.

(2) Krätschmer, W.; Lamb, L. D.; Fostiropoulos, K.; Huffman, D. R. *Nature* **1990**, *347*, 354.

(3) For recent reviews on C_{60}, see: (a) McLafferty, F. W., Ed. *Acc. Chem. Res.* **1992**, *25*, 97. (b) Kroto, H. W. *Angew. Chem., Int. Ed. Engl.* **1992**, *31*, 111. (c) Diederich, F.; Whetten, R. L. *Angew. Chem., Int. Ed. Engl.* **1991**, *30*, 678. (d) Kroto, H. W.; Allaf, A. W.; Balm, S. P. *Chem. Rev.* **1991**, *91*, 1213. (e) Stoddart, J. F. *Angew. Chem., Int. Ed. Engl.* **1991**, *30*, 70. Also see: (f) *Fullerenes*; Hammond, G. S.; Kuck, V. J.; Eds.; ACS Symp. Ser., 481; American Chemical Society: Washington, DC, 1992.

(4) (a) Parker, D. H.; Wurz, P.; Chatterjee, K.; Lykke, K. R.; Hunt, J. E.; Pellin, M. J.; Hemminger, J. C.; Gruen, D. M.; Stock, L. M. *J. Am. Chem. Soc.* **1991**, *113*, 7499. (b) Koch, A. S.; Khemani, K. C.; Wudl, F. *J. Org. Chem.* **1991**, *56*, 4543. (c) Pradeep, T.; Rao, C. N. R. *Mat. Res. Bull.* **1991**, *26*, 1101. (d) Hare, J. P.; Kroto, H. W.; Taylor, R. *Chem. Phys. Lett.* **1991**, *177*, 394. (e) Haufler, R. E.; Conceicao, J.; Chibante, L. P. F.; Chai, Y.; Byrne, N. E.; Flanagan, S.; Haley, M. M.; O'Brien, S. C.; Pan, C.; Xiao, Z.; Billups, W. E.; Ciufolini, M. A.; Hauge, R. H.; Margrave, J. L.; Wilson, L. J.; Curl, R. F.; Smalley, R. E. *J. Phys. Chem.* **1990**, *94*, 8634.

(5) There are other methods of producing C_{60}, most notably from hydrocarbon flames and by the thermal evaporation of carbon, see: (a) Howard, J. B.; McKinnon, J. T.; Makarovsky, Y.; Lafleur, A. L.; Johnson, M. E. *Nature* **1991**, *352*, 139. (b) Peters, G.; Jansen, M. *Angew. Chem., Int. Ed. Engl.* **1992**, *31*, 223.

0022-3263/92/1957-6932$03.00/0

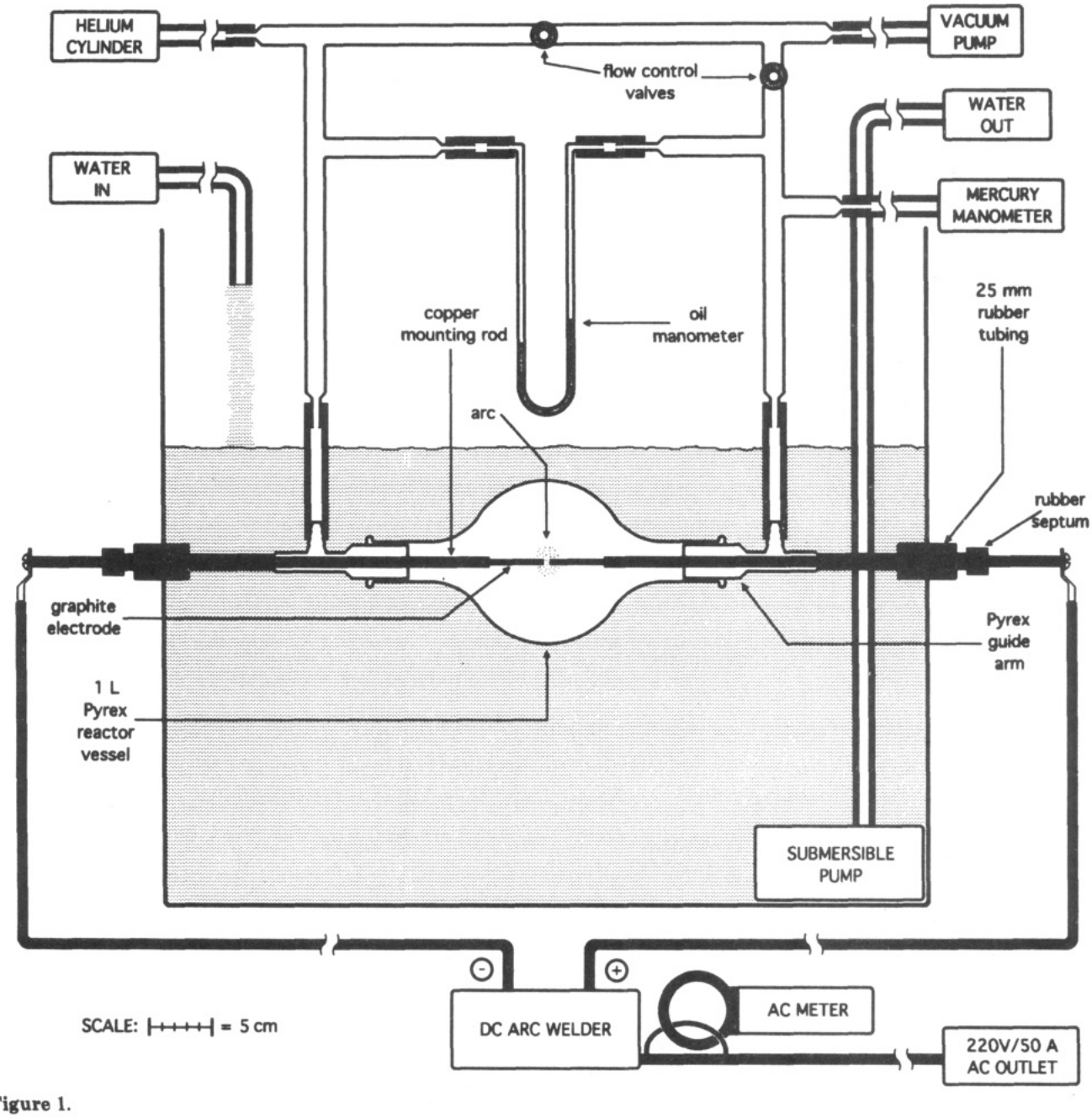

Figure 1.

a no. 2 hole punched through their center. These septa maintain a seal between the sliding copper mounting rod and the end of the Pyrex guide arm. The guide arm's vacuum take off adapters connect, via rubber tubing, to a gas manifold mounted above the reactor vessel (the outside diameter of the manifold tubing is 15 mm).

The entire vessel, except for the ends of the guide arms, is submerged in a cooling water bath made from a plastic storage container.[6] Two holes slightly less than 25 mm in diameter are made in the side of the storage container by heating an appropriately-sized glass tube in a gas flame and melting through the plastic. It is through these holes that the guide arms pass while water leaks are prevented by using rubber gaskets made from a short lengths of 25-mm rubber tubing. A submersible water pump is placed at the bottom of the cooling bath which helps to circulate the cooling (tap) water around the vessel and allows the water to be removed from the bath as quickly as it flows in from a rubber hose at the top of the bath. If the water is not circulated and replenished in this manner, the bath tends to overheat, which can result in the vessel cracking.

The gas manifold above the vessel carefully monitors and controls the atmospheric conditions inside the vessel. Helium flows into the left side of the manifold and the gas is removed from the right sie of the manifold by a vacuum pump. The absolute pressure of gas in the vessel is monitored by a mercury manometer mounted on the right side of the manifold just above the reactor vessel. The pressure difference between the two sides of the vessel is an indication of the direction and magnitude of gas flow through the vessel and is measured by a silicon oil manometer (8 mm o.d.) mounted across the two sides of the manifold. The flow of the gas through the reaction vessel is controlled by two standard high vacuum Teflon-brand plug control valves. The central valve acts as a shunt, directing all or some of the helium flow through the vessel rather than across the top of the manifold. The valve on

(6) These storage containers are available at most department stores for approximately $10 and are made of a flexible plastic similar to plastic garbage containers.

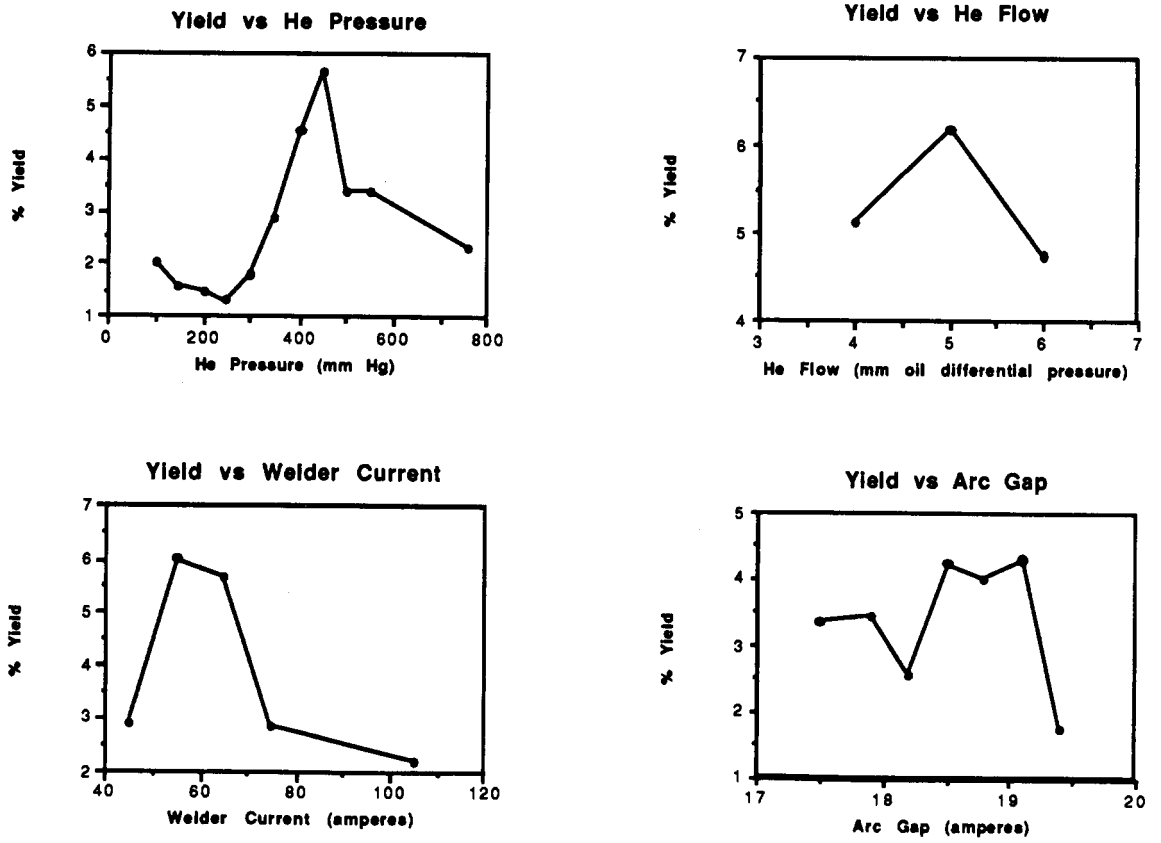

Figure 2.

the right side of the manifold controls the rate of helium flow out of the vessel and thus regulates the sensitivity of the shunt control valve.

The reactor is powered by a variable current AC/DC arc welder which is plugged into a standard 220 V/50 A wall outlet.[7] A clip-on digital AC current meter is attached to the input end of the arc welder to monitor the current.[8]

The apparatus described not only provides us with an inexpensive and easily fabricated fullerene reactor but also gives us the flexibility to adjust and optimize various reaction parameters in order to increase yields. We have determined that there are four easily adjusted parameters that must be maintained for high yields: (1) the absolute pressure, (2) the rate of helium gas flow through the reactor, (3) the current level of the arc as determined by the setting on the arc welding unit, and (4) the arc gap maintained by monitoring the current on the clip-on digital AC current meter. Other workers have dealt with some of these parameters but here we describe the control and optimization of all four parameters simultaneously (Figure 2). Optimization studies were done with inexpensive graphite welding electrodes.[9] We eventually started using high purity graphite electrodes which doubled our yields.[10] Even with this change in electrode type, all the optimized reactor conditions given in Figure 2 hold for both sources of graphite except for the optimal arc gap measured in amperes on the clip-on digital AC current meter.

Helium pressure is the operating parameter that is commonly reported for the synthesis of fullerenes. Our studies have shown that there is a local yield maximum at about 150 mmHg but that the yield optimum occurs at 450 mmHg after going through a yield minimum at 250 mmHg. An optimized operating pressure of 450 mmHg is significantly higher than the operating pressures of 100–200 mmHg normally used by other workers;[3] however, a recent report suggested that optimal pressures for graphitic nanotube formation was in the range of 500 mmHg, similar to our maximum for C_{60} formation.[11] These pressures are monitored by a standard U-shaped mercury manometer and the pressures can be accurately adjusting by the low-pressure valve on the helium regulator.

The next condition that we investigated was that of helium flow through the reactor. By adjusting the flow control valves on the gas manifold and monitoring the differential pressure on the U-shaped silicon oil manometer, one can adjust the helium flow through the reactor from 0 mm (a static helium atmosphere) to greater than 30 mm oil pressure. A differential oil pressure reflects a net helium flow through the reactor from left to right. An optimum flow was found at 5 mm oil pressure. Pressures greater than 6 mm caused the soot to accumulate on the right side of the reactor and blew soot out of the reactor and into the manifold and vacuum lines. Pressures less than 4 mm gave extremely low yields and caused the soot

(7) The arc welder (Lincoln Electric model AC/DC 225/125) was purchased from a local welding supplier and cost approximately $300.

(8) The clip-on digital AC current meter was purchased from a local electronics distributor for approximately $100. The meter is attached around one of the two hot leads of the 220 V power cord attached to the arc welder. One can access these leads by carefully removing the outer power cord covering, exposing three wires, namely, the two colored hot leads and the one white ground lead. Care must be taken to not penetrate the insulation of these inner wires. The current meter is then clipped around one of the exposed hot leads. The metallic portion of the wires should never be exposed.

(9) Standard 3/16 in. copper-clad graphite electrodes (Arcair brand, $0.25/rod) were obtained from a local welding supply center. The copper sheathing was peeled off before use. Technical data sheets on these electrodes showed that a significant amount of the mass consisted of nongraphitic binders that probably caused the lower yields seen in the optimization study graphs.

(10) High quality graphite electrodes (Cat. #AXF-5Q1, $1.92/rod, 6 in. long, 3/16 in. diameter) were obtained from Poco Graphite, Inc., 1601 South State Street, Decatur, TX 76234.

(11) Ebbesen, T. W.; Ajayan, M. *Nature* **1992**, *358*, 220.

to accumulate on the left side of the reactor. Observation of the arc through a modified reactor vessel equipped with a view port[12] revealed that under a static helium atmosphere the arc plume actually flowed from the positive to the negative electrode (this is the direction of the current flow). A slight helium flow in the opposite direction seemed to counteract this current flow and "balanced" the arc so that at the optimum flow of 5 mm, the soot stayed in the center of the reactor vessel rather than flowing out one side or the other.

The welder current was the next parameter that we investigated and it was adjusted to obtain an optimum fullerene yield. Our studies showed that a current of 55 A gave the best yields. Higher current increased graphite rod burn rates but decreased yields.[13] At currents lower than 55 A we had difficulty maintaining an arc.

Finally, varying arc gaps were investigated. Other workers optimized this parameter by setting the arc gap to a level where the arc was "brightest".[14] We sought to find a more objective criteria for determining arc gap and found that monitoring the current draw of the arc with the clip-on digital AC current meter attached to the arc welder was a convenient and reliable way of monitoring this parameter.[8] While using welding grade graphite rods,[9] an optimum arc gap of 2–4 mm (determined visually through the view port)[12] corresponded to a current reading of 18.5–19.0 A on the clip-on digital current meter. Using high purity graphite rods,[10] the optimum arc gap of 2–4 mm corresponded to a current reading of 6.6–7.2 A on the clip-on digital current meter.

A detailed experimental procedure is as follows. The two guide arms were removed from a 110 °C oven, the 25-mm rubber tubing gaskets were slipped onto the end of the arms, the manifold hoses were attached, and the two arm assemblies were inserted through the holes of the empty cooling bath. The reactor vessel was then removed from the oven, the two joints are well-lubricated with silicon grease, and the vessel was mounted between the two guide arms. Adjustments in the guide arms were made to ensure a tight fit between the ground glass joints. Two weighed high purity graphite electrodes[10] (6 in. long) were inserted into the ends of the two copper mounting rods, the rubber septa were slipped over the other ends of the rods, and the rod assemblies were then inserted into the end of the guide arms. The septa were adjusted so that they slip over the end of the guide arm and give a reasonable vacuum seal.[15] The chamber was then evacuated, and the reactor was attached to the arc welder with the screw connections. The cooling bath was filled with tap water and the water flow was adjusted so that when the submersible pump was turned on, there was no net flow of water out of the cooling bath. It is important that the reactor vessel is always covered with water to avoid cracking of the reactor. The system was then kept under 5 mm vacuum[15] for 20 min. Helium was then introduced into the reactor and the pressure was adjusted at the regulator until an absolute pressure of 450 mmHg was obtained as determined by the mercury manometer. The flow control valves were then adjusted until a diffrential pressure of 5 mm was reached in the silicon oil U-tube. The copper mounting rods were pushed in until the two graphite rods were centered in the vessel but were not touching. While wearing rubber gloves and welder's goggles, the arc welder was set to 55 A DC, and the AC current meter and the arc welder were turned on (*CAUTION*).[16] The right copper mounting rod was pushed in slightly so that the graphite electrodes briefly touched and established an arc. This right copper rod was then moved in or out until the current meter read 7.2 A. The rod was allowed to burn until the current meter read 6.6 A at which point the right copper rod was again pushed in until a 7.2-A reading was obtained. This process was then repeated. One only needs to adjust the right copper rod (the positive electrode) because the left electrode is never consumed. It takes from 2–3 min for the graphite rod to burn through the 7.2–6.6-A range. Slag (as observed through the view port of our test apparatus)[12] accumulates on the left electrode and must occasionally (about every 30 min) be removed. This is accomplished by turning off the arc welder, waiting 30 s for the electrodes to cool, and tapping on the left copper mounting rod with a glass rod which knocks the slag off the electrode. Failure to turn off the arc welder and wait for the electrodes to briefly cool before dislodging the slag can cause the vessel to crack when the hot slag hits the bottom of the vessel and induces thermal stresses in the glass. An entire 15-cm electrode was consumed in about 1.25 h. One must be careful to not burn the graphite rod down below 1.5 cm; failure to do this can cause the arc to jump to the copper mounting rod, melting the top of the copper rod and necessitating redrilling of the graphite rod holding hole. Additional graphite electrodes can be burned in the same run by turning off the welder, bringing the reactor up to atmospheric pressure, removing the right mounting rod and replacing the consumed graphite stub with a new rod, re-inserting the mounting rod, pumping the system down to 5 mmHg, bringing the atmosphere back to 450 mmHg, turning the welder back on, and initiating a new arc. One need not disassemble the apparatus nor empty the cooling bath during this procedure. About six rods can be consumed in an 8-h period. If more than eight rods are consumed in a single run, the guide arms tend to clog with soot and the reactor becomes inefficient.

When the run was complete, the reactor was taken apart and the vessel had the joints wiped free of grease with paper towels and hexane. One end of the vessel was capped with a 24/40 rubber septum, the flask was filled with 500 mL of toluene, and then the other end of the vessel was also capped with a 24/40 rubber septum which had a needle inserted in it to avoid pressure build-up in the vessel. The reaction vessel was then carefully shaken to dislodge most of the soot and facilitate suspension of the soot in the toluene. The vessel was then placed in a sonic water bath for 30 min (with the needle pointing up and out of the water). The black soot suspension was then filtered through a pad of Celite-521 in a fritted glass funnel to give a dark red-brown solution of crude fullerenes. The

(12) The apparatus with a view port had an additional 24/40 female joint placed at right angles to the guide arms in the center of the 1-L reaction vessel, directly above the point of the arc. A tube was made with a male 24/40 joint (20-mm diameter, 20-cm long tube including the male joint) at one end and a clear glass window attached to the tube with epoxy at the other end. This tube was inserted into the female joint such that the window points up and out of the water bath. It is through this window that we directly observed the arc. Welder's goggles are used when looking into the port at the arc to avoid eye injury. Use of a view port of this type will easily allow observation of electrodes and slag build-up.

(13) Wudl et al. had similar burn and yield observations when moving to a higher current. See ref 4b.

(14) Parker et al. observed that their optimum arc gap was 4 mm. See ref 4a.

(15) With our apparatus a vaccum of only 5 mmHg can be obtained. The rubber septa are most likely the weak points in our system and cause the leaks which prevents us from obtaining lower pressures.

(16) The apparatus poses risks of electrical shock similar to those risks incurred during ordinary arc welding. Accordingly, rubber gloves should be worn to avoid electrical shock while handling the exposed copper rods. The operator should wear rubber-soled shoes and only one hand should be in contact with the copper rod at any time. To avoid eye injury, welder's goggles should be worn when observing the arc.

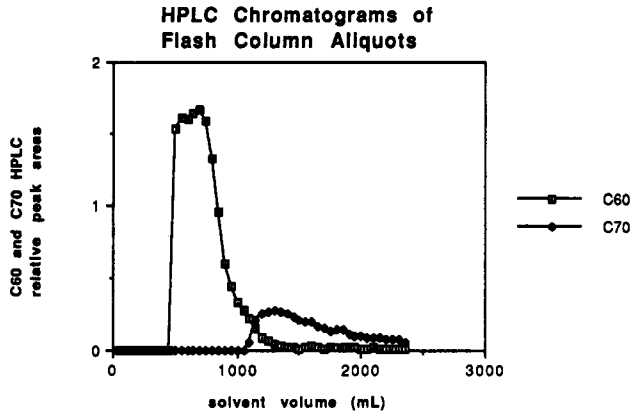

Figure 3.

solvent was removed from the crude fullerene extract by rotary evaporation to give a black powder. The black powder was suspended in diethyl ether and poured onto the top of a small plug of silica gel. The crude fullerenes are insoluble in ether and stay at the top of the column. While at the top of the column, the crude material was washed generously with ether and then flushed through the column with distilled toluene. The discarded ether washings removed the grease residues and the ubiquitous hydrocarbon side products of the fullerene reaction; the silica gel plug also acts as a fine filter to remove any soot that passed through the Celite pad. This filtered crude extract was then concentrated by rotary evaporation and weighed. We have found that this clean-up procedure is necessary for obtaining accurate weights of the crude soluble fullerene extracts and neglect of this type of purification will undoubtedly cause hydrocarbon and/or insoluble particulate to inaccurately enhance the reported crude yields. The weights of the consumed rods and the slag were obtained and subtracted from the initial weights of the rods to give a weight of the graphite that was consumed and converted into soot. The crude yield was then calculated from these values. A typical 1-rod run takes 78 min, burns 2142 mg of graphite, and produces 278 mg of soluble crude fullerenes, giving a crude yield of 13%. Yields reproducibly ranged from 11 to 14%. Thus an 8-h run that consumes six graphite rods will produce ~1.7 g of crude fullerenes from which ~1.0 g of pure C_{60} can be obtained by the following purification procedure.

The crude material was purified on an activated charcoal/silica gel flash column.[17] A slurry of alkaline decolorizing carbon Norit-A (36 g) and silica gel (72 g) in toluene (200 mL) was poured into a typical glass flash chromatography column (38-mm diameter and 40 cm long) that had a cotton plug at the bottom of the column. The slurry was allowed to settle as the solvent *above* the stationary phase was allowed to drain under a 7.5 psi N_2 head pressure applied at the top of the column.[18] The stationary phase must not be allowed to become solvent free or else cracking of the stationary phase can occur. A saturated toluene (400 mL) solution of crude fullerenes (1.85 g) extracted from carbon arc soot was slowly poured onto the top of the Norit-A/silica gel stationary phase. A 7.5 psi N_2 head pressure was applied, thus providing a ~16 mL/min elution rate. The deep purple-colored solution containing C_{60} started to elute from the column after 37 min. After 36 min more, the eluant was only faintly purple and collection of a second faction was then begun. The total volume of toluene needed for obtaining the C_{60} fraction (first fraction) was ~600 mL. After 3 min more, a red-brown band characteristic of C_{70} started to elute. A graph of aliquots analyzed by HPLC[19] shows the relative concentrations of C_{60} and C_{70} versus solvent volume (Figure 3). Removal of the solvent from the purple fraction afforded 1.16 g of crystalline C_{60} (63% of a possible 75% of C_{60} in extractable fullerenes) that was >99% pure by HPLC.[17,19] This represents a net yield of about 8.5% pure C_{60} based on the weight of the graphite consumed.[20] While the second band eluted from the column was red-brown, it did contain some C_{60}. One more smaller chromatographic run on the initial red-brown portion afforded 74 mg more of C_{60} and 120 mg of a sample that was ~1:10 in C_{60}:C_{70} as judged by HPLC analysis.[18] Thus the combined yield of purified C_{60} after two columns was 67% of a possible 75% of C_{60} in extractable fullerenes.

Although we illustrated this purification procedure with 1.85 g of extractable fullerenes, it worked equally well on a smaller scale using the proportionately smaller stationary phases and solvent volumes. Norit-A alone as the stationary phase without silica gel as a co-phase worked excellently for C_{60} separations on smaller scales (i.e., 100 mg of crude fullerenes with 2.0 g of Norit-A); however, the silica gel prevents cracking of the stationary phase in the larger columns and allows for higher flow rates.

In summary, we have described and inexpensive and easily fabricated fullerene reactor of the arc discharge type. The apparatus described allows one to control various reaction parameters and optimization of the parameters gives reproducible runs of 11–14% crude yield. The crude material is purified on a activated charcoal/silica gel column to give a net pure C_{60} yield of 8.5% from consumed graphite.[20]

Acknowledgment. This research was funded by the Department of the Navy, Office of the Chief of Naval Research, Young Investigator Award Program (1989–92), the National Science Foundation (RII-8922165, DMR-9158315), and generous industrial contributors to the NSF Presidential Young Investigator Award (1991–96) for J. M.T.: Hercules Incorporated, IBM Corporation, Ethyl Corporation, and the Shell Development Company. W. A.S. thanks NASA and the American Vacuum Society for scholarships. We thank Dr. Nick Griffith of the Aluminum Company of America for providing us with alumina for the comparison studies.

(17) Alkaline decolorizing carbon Norit-A was purchased from Fisher Scientific Company. Flash chromatography grade silica gel 60 (230–400-mesh ASTM, 0.040–0.063 mm particle size) was purchased from EM Science. A detailed description of this purification method and the purity of the C_{60} and C_{70} obtained was recently described. See: Scrivens, W. A.; Bedworth, P. V.; Tour, J. M. *J. Am. Chem. Soc.* **1992**, *114*, 7917.

(18) *CAUTION*: Though we experienced no rupture of the glass under 7.5–10 psi pressures, we recommend utilization of this procedure behind a protective transparent shield to prevent injury if a rupture should occur.

(19) HPLC was done using an Alltech Econosphere silica gel column (250 mm × 4.6 mm i.d.) with 2% toluene in hexane at 1 mL/min using UV detection at 284 nm. The crude material showed a mixture of C_{60}, C_{70}, C_{84}, and possibly other higher fullerenes in a peak area ratio of 58.0, 38.9, 1.6, and 1.5, respectively. The retention times were 5.1, 5.9, 6.6, and 7.4 min, respectively, with base-line separation. Thus, at 284 nm, the extinction coefficient of C_{70} appears to be greater than that of C_{60}, therefore skewing detection in favor of C_{70}.

(20) In summary, 2142 mg of graphite consumed from one rod yields 278 mg of crude fullerenes = 13% (generally 11–14%) crude yield or yield of soluble extract. At 2142 mg of graphite consumed per rod × 6 rods per 8 h = 12.9 g of graphite that can be consumed in this apparatus per 8 h; 12.9 g of graphite consumed × (11–14% crude yield) = 1.42–1.81 g of crude fullerenes per 8 h; 1.42–1.81 g × 63% chromatographic recovery of pure C_{60} = 0.89 g to 1.14 g of pure C_{60}; 0.89–1.14 g of pure C_{60}/12.9 g of graphite consumed = 6.9–8.8% of pure C_{60} obtainable based on the mass of graphite consumed.

41. Sander, S. P., Friedl, R. R. & Yung, Y. L. *Science* **245,** 1095–1098 (1989).
42. Trolier, M., Mauldin, R. L. III & Ravishankara, A. R. *J. phys. Chem.* **94,** 4896–5001 (1990).
43. Proffitt, M. H. *et al. J. geophys. Res.* **94,** 16547–16556 (1989).
44. Schoeberl, M. R. *et al. J. geophys. Res.* **94,** 16815–16846 (1989).
45. Yung, Y. L., Allen, M., Crisp, D., Zurek, R. W. & Sander, S. P. *Science* **248,** 721–724 (1990).
46. *J. geophys. Res.* **94,** Nos 9 and 14 (1989).
47. Barrett, J. W. *et al. Nature* **336,** 455–458 (1988).
48. Garcia, R. R. & Solomon, S. *J. geophys. Res.* **88,** 1378–1400 (1983).
49. Jones, R. L. *et al. J. geophys. Res.* **94,** 11529–11558 (1989).
50. Anderson, J. G., Brune, W. H., Toohey, D. W. & Proffitt, N. H. *Science* (in the press).
51. Rodriguez, J. M., Ko, M. K. W. & Sze, N. D. *Geophys. Res. Lett.* **13,** 1292–1295 (1986).
52. Solomon, S., Mount, G. H., Sanders, R. W. & Schmeltekopf, A. L. *J. geophys. Res.* **92,** 8329–8338 (1987).
53. Wahner, A. *et al. J. geophys. Res.* **94,** 11405–11411 (1989).
54. Farmer, C. B., Toon, G. C., Shaper, P. W., Blavier, J. F. & Lowes, L. L. *Nature* **329,** 126–130 (1987).
55. Coffey, M. T., Mankin, W. G. & Goldman, A. *J. geophys. Res.* **94,** 16597–16614 (1989).
56. Toon, G. C. *et al. J. geophys. Res.* **94,** 16571–16596 (1989).
57. Anderson, J. G. *et al. J. geophys. Res.* **94,** 11480–11520 (1989).
58. McElroy, M. B. & Salawitch, R. J. *Planet. Space Sci.* **37,** 1653–1672 (1989).
59. Solomon, S., Sanders, R. W., Carroll, M. A. & Schmeltekof, A. L. *J. geophys. Res.* **94,** 11393–11404 (1989).
60. Solomon, S., Sanders, R. W. & Miller, H. L. *J. geophys. Res.* (in the press).
61. Austin, J. *et al. J. geophys. Res.* **94,** 16717–16736 (1989).
62. Watterson, I. G. & Tuck, A. F. *J. geophys. Res.* **94,** 16511–16526 (1989).
63. Tuck, A. F. *J. geophys. Res.* **94,** 11687–11737 (1989).
64. Hartmann, D. L. *et al. J. geophys. Res.* **94,** 16779–16796 (1989).
65. McCormick, M. P., Zawodny, J. M., Veiga, R. E., Larsen, J. C. & Wang, P. H. *Planet. Space Sci.* **37,** 1567–1586 (1989).
66. Proffitt, M. H. *et al. J. geophys. Res.* **94,** 16797–16814 (1989).
67. Rodriguez, J. M., Ko, M. K. W. & Sze, N. D. *Geophys. Res. Lett.* **17,** 255–258 (1990).
68. Deshler, T., Hofmann, D. J., Hereford, J. V. & Sutter, C. B. *Geophys. Res. Lett.* **17,** 151–154 (1990).
69. Garcia, R. R. & Solomon, S. *Geophys. Res. Lett.* **14,** 848–851 (1987).
70. Ko, M. K. W. *et al. J. geophys. Res.* **94,** 16705–16716 (1989).
71. Blake, D. R. & Rowland, F. S. *Science* **239,** 1129–1131 (1988).
72. Angell, J. K. *J. Clim.* **1,** 1296–1304 (1988).
73. Trenberth, K. E. & Olson, J. G. *J. Clim.* **2,** 1196–1206 (1989).
74. Newman, P. A. & Randel, W. J. *J. geophys. Res.* **93,** 12585–12606 (1988).
75. Poole, L. R., Solomon, S., McCormick, M. P. & Pitts, M. C. *Geophys. Res. Lett.* **16,** 1157–1160 (1989).
76. Shine, K. P. *Geophys. Res. Lett.* **13,** 1331–1334 (1986).
77. Atkinson, R. J., Matthews, W. A., Newman, P. A. & Plumb, R. A. *Nature* **340,** 290–294 (1989).
78. Murphy, D. M. *et al. J. geophys. Res.* **94,** 11669–11686 (1989).
79. Tolbert, M. A., Rossi, M. J. & Golden, D. M. *Geophys. Res. Lett.* **15,** 851–853 (1988).
80. Mozurkewich, M. & Calvert, J. G. *J. geophys. Res.* **93,** 15889–15897 (1988).
81. Hofmann, D. J. & Solomon, S. *J. geophys. Res.* **94,** 5029–5042 (1989).
82. *Geophys. Res. Lett.* **17,** No. 4 (1990).
83. McKenna, D. S. *et al. Geophys. Res. Lett.* **17,** 553–556 (1990).
84. Nagatani, R. M., Miller, A. J., Gelman, M. E. & Newman, P. A. *Geophys. Res. Lett.* **17,** 333–336 (1990).

ACKNOWLEDGEMENTS. I thank D. W. Fahey, R. R. Garcia, G. Huebler, R. L. Jones, D. S. McKenna, D. M. Murphy, A. O'Neill, L. R. Poole, A. R. Ravishankara and A. F. Tuck for comments.

ARTICLES

Solid C_{60}: a new form of carbon

W. Krätschmer*, Lowell D. Lamb†, K. Fostiropoulos* & Donald R. Huffman†

* Max-Planck-Institut für Kernphysik, 6900 Heidelberg, PO Box 103980, Germany
† Department of Physics, University of Arizona, Tucson, Arizona 85721, USA

A new form of pure, solid carbon has been synthesized consisting of a somewhat disordered hexagonal close packing of soccer-ball-shaped C_{60} molecules. Infrared spectra and X-ray diffraction studies of the molecular packing confirm that the molecules have the anticipated 'fullerene' structure. Mass spectroscopy shows that the C_{70} molecule is present at levels of a few per cent. The solid-state and molecular properties of C_{60} and its possible role in interstellar space can now be studied in detail.

FOLLOWING the observation that even-numbered clusters of carbon atoms in the range C_{30}–C_{100} are present in carbon vapour[1], conditions were found[2–4] for which the C_{60} molecule could be made dominant in the large-mass fraction of vapourized graphite. To explain the stability of the molecule, a model was proposed of an elegant structure in which the carbon atoms are arranged at the 60 vertices of a truncated icosahedron, typified by a soccer ball. The structure, dubbed buckminsterfullerene[2] because of its geodesic nature, has been the subject of several theoretical stability tests[5,6] and has been discussed widely in the literature. Calculations of many physical properties have been made, including electron energies[7–9], the optical spectrum[9], vibrational modes[10–15], and the electric and magnetic properties[16,17]. There has been speculation on the possible chemical and industrial uses of C_{60} (ref. 2), and on its importance in astrophysical environments[18–20]. Until now, it has not been possible to produce sufficient quantities of the material to permit measurement of the physical properties, to test the theoretical calculations, or to evaluate the possible applications.

Some of us have recently reported evidence[21,22] for the presence of the C_{60} molecule in soot condensed from evaporated graphite. The identification was based primarily on the observed isotope shifts of the infrared absorptions when ^{12}C was replaced by ^{13}C, and on comparison of the observed features with theoretical predictions. The measured infrared and ultraviolet absorption bands were superimposed on a rather large continuum background absorption from the graphitic carbon which comprised $\geq$95% of the sample. Here we report how to extract the carrier of the features from the soot, how to purify it, and evidence that the material obtained is in fact primarily C_{60}.

Method of production

The starting material for our process is pure graphitic carbon soot (referred to below as simply soot) with a few per cent by weight of C_{60} molecules, as described in refs 21, 22. It is produced by evaporating graphite electrodes in an atmosphere of ~100 torr of helium. The resulting black soot is gently scraped from the collecting surfaces inside the evaporation chamber and dispersed in benzene. The material giving rise to the spectral features attributed to C_{60} dissolves to produce a wine-red to brown liquid, depending on the concentration. The liquid is then separated from the soot and dried using gentle heat, leaving a residue of dark brown to black crystalline material. Other non-polar solvents, such as carbon disulphide and carbon tetrachloride, can also dissolve the material. An alternative concentration procedure is to heat the soot to 400 °C in a vacuum or in an inert atmosphere, thus subliming the C_{60} out of the soot (W. Schmidt, personal communication). The sublimed coatings are brown to grey, depending on the thickness. The refractive index in the near-infrared and visible is about two. To purify the material, we recommend removing the ubiquitous hydrocarbons before the concentration procedure is applied (for example, by washing the initial soot with ether). Thin films and powder samples of the new material can be handled without special precautions and seem to be stable in air for at least several weeks, although there does seem to be some deterioration with time for reasons that are as yet unclear. The material can be

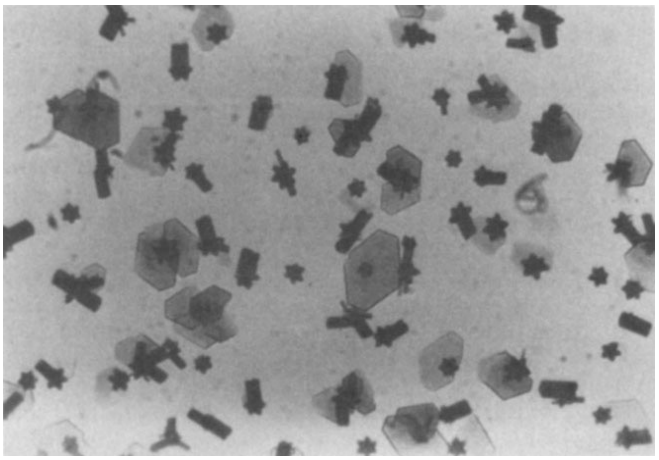

FIG. 1 Transmission micrograph of typical crystals of the C_{60} showing thin platelets, rods and stars of hexagonal symmetry.

sublimed repeatedly without decomposition. Using the apparatus described, one person can produce of the order of 100 mg of the purified material in a day.

Studies by optical microscopy of the material left after evaporating the benzene show a variety of what appear to be crystals—mainly rods, platelets and star-like flakes. Figure 1 shows a micrograph of such an assemblage. All crystals tend to exhibit six-fold symmetry. In transmitted light they appear red to brown in colour; in reflected light the larger crystals have a metallic appearance whereas the platelets show interference colours. The platelets can be rather thin and are thus ideally suited for electron-diffraction studies in an electron microscope (see the inset in Fig. 3).

Mass spectroscopy

The material has been analysed by mass spectrometry at several facilities. All mass spectra have a strong peak at mass 720 a.m.u., the mass of C_{60}. Significant differences in the spectra occur only at masses lower than 300 a.m.u. Most of these differences seem to originate from the different ionization techniques and in the different methods of desorbing molecules from the sample. Mass spectra recorded at low and high resolution are shown in Fig. 2. The spectra were obtained using a time-of-flight secondary-ion mass spectrometer[23] and a C_{60}-coated stainless-steel plate. In the mass range above 300 a.m.u., the spectrum is dominated by C_{60} ions and its fragments (even-numbered clusters of atomic carbon), and C_{70} ions. In this sample, the ratio of C_{70} to C_{60} is ~0.1. The high-resolution mass spectrum shows approximately the expected isotope pattern for C_{60}. The increasing background in the low-resolution mass spectrum is not produced by the sample—such backgrounds also occur in blank measurements on uncoated stainless-steel substrates.

So far, the cleanest mass spectra have been obtained when the material was evaporated and ionized in the vapour phase by electrons. In such spectra the low-mass background is substantially reduced and the entire mass spectrum is dominated by C_{60} ions and its fragments. The ratio of C_{70} to C_{60} in these mass spectra is ~0.02 and seems to be smaller than that shown in Fig. 2. Both ratios are of the order of those reported from laser-evaporation experiments[2,3]. We assume, as previously suggested[24], that the C_{70} molecule also has a closed-cage structure, either elongated[24] or nearly spherical[25]. Further details of the mass spectroscopy of the new material will be published elsewhere.

Structure

To determine if the C_{60} molecules form a regular lattice, we performed electron and X-ray diffraction studies on the individual crystals and on the powder. A typical X-ray diffraction pattern of the C_{60} powder is shown in Fig. 3. To aid in comparing the electron diffraction results with the X-ray results we have inset the electron diffraction pattern in Fig. 3. From the hexagonal array of diffraction spots indexed as shown in the figure, a d spacing of 8.7 Å was deduced corresponding to the (100) reciprocal lattice vector of a hexagonal lattice. The most obvious correspondence between the two types of diffraction is between the peak at 5.01 Å of the X-ray pattern and the (110) spot of the electron diffraction pattern, which gives a spacing of ~5.0 Å. Assuming that the C_{60} molecules are behaving approximately as spheres stacked in a hexagonal close-packed lattice with a c/a ratio of 1.633, d spacings can be calculated. The results are shown in Table 1. The values derived from this interpretation are $a = 10.02$ Å and $c = 16.36$ Å. The nearest-neighbour distance is thus 10.02 Å. For such a crystal structure the density is calculated to be 1.678 g cm^{-3}, which is consistent with the value of 1.65 ± 0.05 g cm^{-3} determined by suspending crystal samples in aqueous $GaCl_3$ solutions of known densities. Although the agreement shown in Table 1 is good, the absence of the characteristically strong (101) diffraction of the hexagonal close-packed structure, and the broad continuum in certain regions suggest that the order is less than

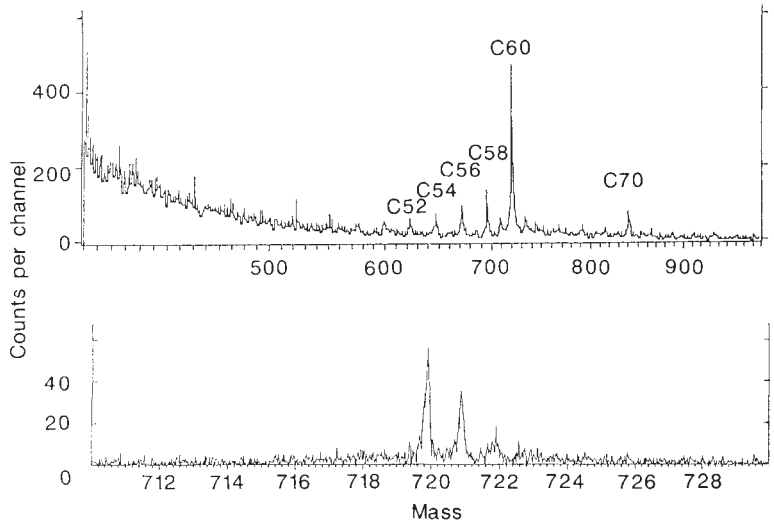

FIG. 2 Low-resolution (top) and high-resolution time-of-flight mass spectra of positive ions obtained from coatings of solid C_{60}. A 5-keV Ar^+ ion beam was used to sputter and ionize the sample. The isotope pattern (bottom) is approximately that expected for C_{60} molecules composed of ^{12}C and ^{13}C isotopes of natural abundance.

TABLE 1 X-ray diffraction results

Measured 2θ (deg)	Measured d spacing (Å)	Calculated d spacing (Å)	Assignment (hkl)
10.2 shoulder	8.7	8.68	(100)
10.81	8.18	8.18	(002)
		7.68	(101)
17.69	5.01	5.01	(110)
20.73	4.28	4.28	(112)
21.63	4.11	4.09	(004)
28.1	3.18	3.17	(114)
30.8	2.90	2.90	(300)
32.7	2.74	2.73	(006)

Assignments for a hexagonal lattice using $a=10.02$ Å, $c=16.36$ Å. $(1/d^2)=\frac{4}{3}[(h^2+hk+k^2)/a^2]+l^2/c^2$.

perfect. Further, X-ray diffraction patterns from carefully grown crystals up to 500 μm in size with well developed faces yielded no clear spot pattern (in contrast to the electron diffraction pattern on micrometre-sized crystals). It therefore appears that these larger crystals do not exhibit long-range periodicity in all directions.

A likely explanation for these facts lies in the disordered stacking of the molecules in planes normal to the c axis. It is well known that the positions taken by spheres in the third layer of stacking determines which of the close-packed structures occurs, the stacking arrangement in a face-centred cubic structure being ABCABC... whereas that in a hexagonal close-packed structure is ABABAB... If the stacking sequence varies, the X-ray lines owing to certain planes will be broadened by the disorder whereas other lines will remain sharp. Such disordered crystalline behaviour was observed long ago in the hexagonal close-packed structure of cobalt[26–28] where X-ray diffraction lines such as (101), (102) and (202) were found to be substantially broadened by the stacking disorder. Reflections from planes such as (002) remain sharp because these planes have identical spacings in the face-centred cubic and hexagonal close-packed structures. For the planes producing broadened diffraction peaks because of this kind of disorder, the following condition for the Miller indices (hkl) has been shown to apply[27,29]: $h-k=3t\pm1$ (where t is an integer) and $l\neq0$. None of these broadened reflections are apparent in the X-ray pattern of Fig. 3. This may explain the weakness of the characteristically strong (101) peak. Whether or not this stacking disorder is related to the presence of the possibly elongated C_{70} molecule has yet to be determined.

In small crystals at least, the C_{60} molecules seem to assemble themselves into a somewhat ordered array as if they are effectively spherical, which is entirely consistent with the hypothesis that they are shaped like soccer balls. The excess between the nearest-neighbour distance (10.02 Å) and the diameter calculated for the carbon cage itself (7.1 Å) must represent the effective van der Waals diameter set by the repulsion of the π electron clouds extending outward from each carbon atom. Because the van der Waals diameter of carbon is usually considered to be 3.3–3.4 Å the packing seems a little tighter than one might expect for soccer-ball-shaped C_{60} molecules. The reason for this has not yet been determined.

In summary, our diffraction data imply that the substance isolated is at least partially crystalline. The inferred lattice constants, when interpreted in terms of close-packed icosahedral C_{60}, yield a density consistent with the measured value. Further evidence that the molecules are indeed buckminsterfullerene and that the solid primarily consists of these molecules comes from the spectroscopic results.

Spectroscopy

The absorption spectra of the graphitic soot[21,22] showed evidence for the presence of C_{60} in macroscopic quantities. Following the purification steps described above the material can be studied spectroscopically with the assurance that the spectra are dominated by C_{60}, with some possible effects from C_{70}. Samples were prepared for spectroscopy by subliming pure material onto transparent substrates for transmission measurements. Depending on the pressure of helium in the sublimation chamber, the nature of the coatings can range from uniform films (at high vacuum) to coatings of C_{60} smoke (sub-micrometre microcrystalline particles of solid C_{60}) with the particle size depending to some extent on the pressure.

Figure 4 shows the transmission spectrum of an ~2-μm-thick C_{60} coating on a silicon substrate. The infrared bands are at the same positions as previously reported[21,22], with the four most intense lines at 1,429, 1,183, 577 and 528 cm^{-1}; here, however, there is no underlying continuum remaining from the soot. In many of our early attempts to obtain pure C_{60}, there was a strong band in the vicinity of 3.0 μm, which is characteristic of a CH-stretching mode. After much effort this contaminant was successfully removed by washing the soot with ether and using distilled benzene in the extraction. The spectrum in Fig. 4 was obtained when the material cleaned in such a manner was sublimed under vacuum onto the substrate. The spectrum shows

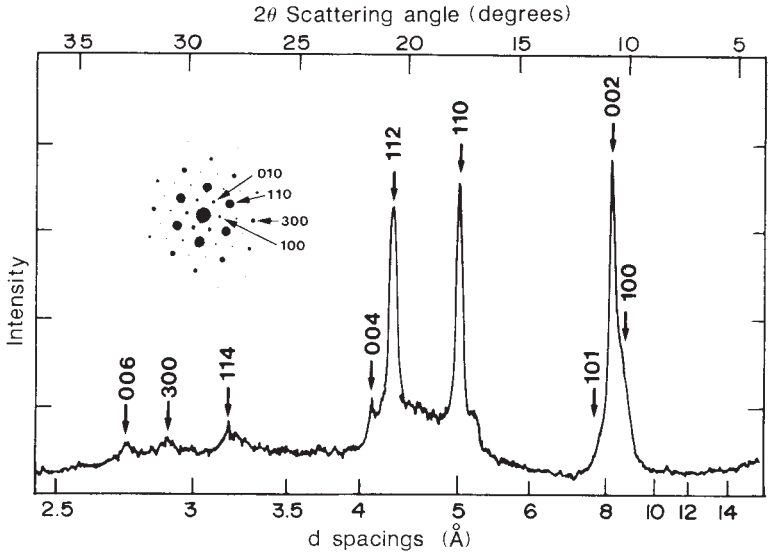

FIG. 3 X-ray diffraction pattern of a microcrystalline powder of C_{60}. Inset (upper left) is a single-crystal electron diffraction pattern indexed with Miller indices compatible with the X-ray pattern. The pattern is from a thin platelet such as those in Fig. 1 with the electron beam perpendicular to the flat face.

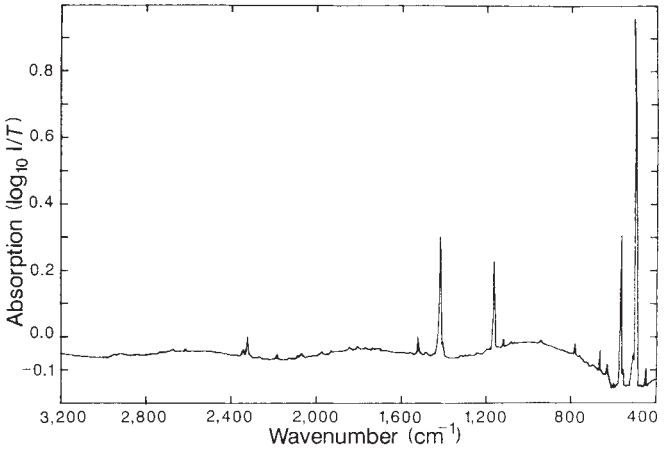

FIG. 4 Infrared absorption spectrum of a coating, ~2 μm thick, of solid C_{60} on a silicon substrate, referenced to a clean silicon substrate. Apparent negative absorptions are due to the coating acting in part as a non-reflecting layer.

very little indication of CH impurities. Vibrational modes to compare with the measured positions of the four strong bands have been calculated by several workers[10–15]. As noted previously, the presence of only four strong bands is expected for the free, truncated icosahedral molecule with its unusually high symmetry. Also present are a number of other weak infrared lines which may be due to other causes, among which may be absorption by the C_{70} molecule or symmetry-breaking produced (for example) by isotopes other than ^{12}C in the C_{60} molecule or by mutual interaction of the C_{60} molecules in the solid. Weaker features at ~2,330 and 2,190 cm^{-1}, located in the vicinity of the free CO_2 and CO stretching modes, may imply some attachment of the CO_2 or CO to a small fraction of the total number of C_{60} molecules. Another notable feature is the peak at 675 cm^{-1}, which is weak in the thin-film substrates but almost as strong as the four main features in the crystals. We suspect that this vibrational mode may be of solid state rather than molecular origin.

Figure 5 shows an absorption spectrum taken on a uniform film coated on a quartz glass substrate. The ultraviolet features are no longer obscured by the graphitic carbon background as in our previous spectra[22]. Broad peaks at 216, 264 and 339 nm dominate the spectra. Weaker structures show up in the visible, including a plateau between ~460 and 500 nm and a small peak near 625 nm. At the bottom of Fig. 5 we have shown positions

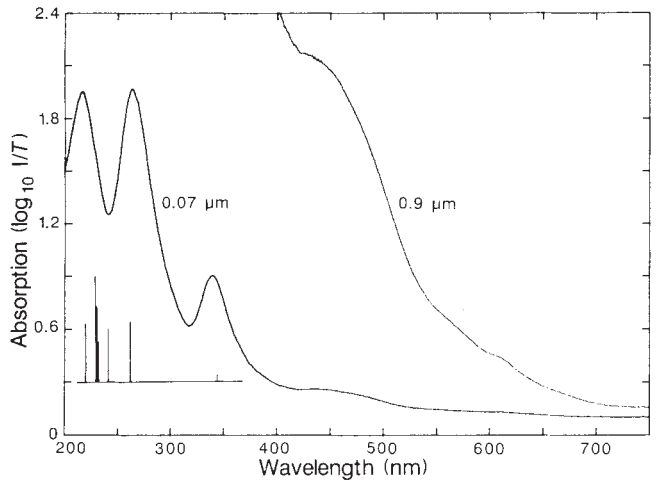

FIG. 5 Visible–ultraviolet absorption spectra of two thicknesses of solid C_{60} on quartz. The calculated[9] positions and relative oscillator strengths for allowed transitions of C_{60} are shown on the bottom.

and relative oscillator strengths taken from Larsson, Volosov and Rosén[9] calculated for the C_{60} molecule. They also reported a variety of forbidden bands with the lowest energy ones in the vicinity of 500 nm. There seems to be a rough correspondence between our measurements on solid films and the allowed transitions predicted for the molecule. The possibility exists, however, that one or more of the absorption features shown in Fig. 5 are due to C_{70}. We still do not observe a band at 386 nm in our films, as observed[30] using a laser depletion spectroscopy method and attributed to the C_{60} molecule. Quite similar spectra to that in Fig. 5 have been recorded for microcrystalline coatings deposited at helium pressures of 100 torr, for example. The peaks occur at the slightly shifted positions of 219, 268 and 345 nm.

Possible interstellar dust

The original stimulus for the work[2] that led to the hypothesis of the soccer-ball-shaped C_{60} molecule, buckminsterfullerene, was an interest in certain unexplained features in the absorption and emission spectra of interstellar matter. These include an intense absorption band at 217 nm which has long been attributed to small particles of graphite[31], a group of unidentified interstellar absorption bands in the visible that have defied explanation for more than 70 years[31,32], and several strong emission bands attributed to polycyclic aromatic hydrocarbons[33,34]. Based on the visible and infrared absorption spectra of Figs 4 and 5, we do not see any obvious matches with the interstellar features. The ultraviolet band at 216–219 nm has a similar peak wavelength to an interstellar feature, although the other strong bands of the spectrum have no interstellar counterparts. As the influence of C_{70} absorptions on the spectrum is not yet known, a conclusive comparison with the 217-nm interstellar band is difficult. We note that the visible–ultraviolet spectrum presented here is characteristic of a solid, rather than of free molecules. In addition, these new results do not relate directly to absorption in the free C_{60}^+ molecular ion, which has been envisaged[19] to explain the diffuse interstellar bands. Nevertheless, these data should now provide guidance for possible infrared detection of the C_{60} molecule, if it is indeed as ubiquitous in the cosmos as some have supposed.

Summary

To our method for producing macroscopic quantities of C_{60}, we have added a method for concentrating it in pure solid form. Analyses including mass spectroscopy, infrared spectroscopy, electron diffraction and X-ray diffraction leave little doubt that we have produced a solid material that apparently has not been reported previously. We call the solid fullerite as a simple extension of the shortened term fullerene, which has been applied to the large cage-shaped molecules typified by buckminsterfullerene (C_{60}). The various physical and chemical properties of C_{60} can now be measured and speculations concerning its potential uses can be tested. □

Received 7 August; accepted 7 September 1990.

1. Rohlfing, E. A., Cox, D. M. & Kaldor, A. *J. chem. Phys.* **81,** 3322–3330 (1984).
2. Kroto, H. W., Heath, J. R., O'Brien, S. C., Curl, R. F. & Smalley, R. E. *Nature* **318,** 162–163 (1985).
3. Zhang, Q. L. *et al. J. phys. Chem.* **90,** 525–528 (1986).
4. Liu, Y. *et al. Chem. Phys. Lett.* **126,** 215–217 (1986).
5. Newton, M. D. & Stanton, R. E. *J. Am. chem. Soc.* **108,** 2469–2470 (1986).
6. Lüthi, H. P. & Almlöf, J. *Chem. Phys. Lett.* **135,** 357–360 (1987).
7. Satpathy, S. *Chem. Phys. Lett.* **130,** 545–550 (1986).
8. Haddon, R. C., Brus, L. E. & Raghavachari, K. *Chem. Phys. Lett.* **125,** 459–464 (1986).
9. Larsson, S., Volosov, A. & Rosén, A. *Chem. Phys. Lett.* **137,** 501–504 (1987).
10. Wu, Z. C., Jelski, D. A. & George, T. F. *Chem. Phys. Lett.* **137,** 291–294 (1987).
11. Stanton, R. E. & Newton, M. D. *J. phys. Chem.* **92,** 2141–2145 (1988).
12. Weeks, D. E. & Harter, W. G. *Chem. Phys. Lett.* **144,** 366–372 (1988).
13. Weeks, D. E. & Harter, W. G. *J. chem. Phys.* **90,** 4744–4771 (1989).
14. Elser, V. & Haddon, R. C. *Nature* **325,** 792–794 (1987).
15. Slanina, Z. *et al. J. molec. Struct.* **202,** 169–176 (1989).
16. Fowler, P. W., Lazzeretti, P. & Zanasi, R. *Chem. Phys. Lett.* **165,** 79–86 (1990).
17. Haddon, R. C. & Elser, V. *Chem. Phys. Lett.* **169,** 362–364 (1990).
18. Kroto, H. *Science* **242,** 1139–1145 (1988).
19. Kroto, H. W. in *Polycyclic Aromatic Hydrocarbons and Astrophysics* (eds Léger, A. *et al.*) 197–206 (Reidel, Dordrecht, 1987).

20. Léger, A., d'Hendecourt, L., Verstraete, L. & Schmidt, W. *Astr. Astrophys.* **203,** 145–148 (1988).
21. Krätschmer, W., Fostiropoulos, K. & Huffman, D. R. in *Dusty Objects in the Universe* (eds Bussoletti, E. & Cittone, A. A.) (Kluwer, Dordrecht, in the press).
22. Krätschmer, W., Fostiropoulos, K. & Huffman, D. R. *Chem. Phys. Lett.* **170,** 167–170 (1990).
23. Steffens, P., Niehuis, E., Friese, T. & Benninghoven, A. *Ion Formation from Organic Solids* (ed. Benninghoven, A.) Ser. chem. Phys. Vol. 25, 111–117 (Springer-Verlag, New York, 1983).
24. Kroto, H. W. *Nature* **329,** 529–531 (1987).
25. Schmalz, T. G., Seitz, W. A., Klein, D. J. & Hite, G. E. *J. Am. chem. Soc.* **110,** 1113–1127 (1988).
26. Hendricks, S. B., Jefferson, M. E. & Schultz, J. F. *Z. Kristallogr.* **73,** 376–380 (1930).
27. Edwards, O. S., Lipson, H. & Wilson, A. J. C. *Nature* **148,** 165 (1941).
28. Edwards, O. L. & Lipson, H. *Proc. R. Soc.* A**180,** 268–277 (1942).
29. Houska, C. R., Averbach, B. L. & Cohen, M. *Acta Metal.* **8,** 81–87 (1960).
30. Heath, J. R., Curl, R. F. & Smalley, R. E. *J. chem. Phys.* **87,** 4236–4238 (1987).
31. Huffman, D. R. *Adv. Phys.* **26,** 129–230 (1977).
32. Herbig, E. *Astrophys. J.* **196,** 129–160 (1975).
33. Léger, A. & Puget, J. L. *Astr. Astrophys. Lett.* **137,** L5–L8 (1984).
34. Allamandola, L. J., Tielens, A. G. & Barker, J. R. *Astrophys. J.* **290,** L25–L28 (1985).

ACKNOWLEDGEMENTS. W.K. and K.F. thank our colleagues F. Arnold, J. Kissel, O. Möhler, G. Natour, P. Sölter, H. Zscheeg, H. H. Eysel, B. Nuber, W. Kühlbrandt, M. Rentzea and J. Sawatzki. L.D.L. and D.R.H. thank our colleagues J. T. Emmert, D. L. Bentley, W. Bilodeau, K. H. Schramm and D. R. Luffer. D.R.H. thanks the Alexander von Humboldt Stiftung for a senior US Scientist award. We also thank H. W. Kroto and R. F. Curl for discussions.

Expression of cystic fibrosis transmembrane conductance regulator corrects defective chloride channel regulation in cystic fibrosis airway epithelial cells

Devra P. Rich, Matthew P. Anderson, Richard J. Gregory*, Seng H. Cheng*, Sucharita Paul*, Douglas M. Jefferson†, John D. McCann, Katherine W. Klinger‡, Alan E. Smith* & Michael J. Welsh§

Howard Hughes Medical Institute, Departments of Internal Medicine and Physiology and Biophysics, University of Iowa College of Medicine, Iowa City, Iowa 52242, USA
* Genzyme Corporation and ‡ IG Laboratories Inc., One Mountain Road, Framingham, Massachusetts 01701, USA
† Department of Physiology, Tufts University School of Medicine, and Departments of Pediatrics and Medicine, New England Medical Center, Boston, Massachusetts 02111, USA

The cystic fibrosis transmembrane conductance regulator (CFTR) was expressed in cultured cystic fibrosis airway epithelial cells and Cl^- channel activation assessed in single cells using a fluorescence microscopic assay and the patch-clamp technique. Expression of CFTR, but not of a mutant form of CFTR (ΔF508), corrected the Cl^- channel defect. Correction of the phenotypic defect demonstrates a causal relationship between mutations in the CFTR gene and defective Cl^- transport which is the hallmark of the disease.

CYSTIC fibrosis (CF), the most common lethal genetic disease in Caucasians[1], is characterized by abnormal electrolyte transport in several organs, including lung, sweat gland, intestine and pancreas[1,2]. Defective regulation of the apical membrane Cl^- channels that control the rate of transepithelial Cl^- transport is well documented in CF epithelia[3–5]. In normal airway epithelia, Cl^- channels are activated (opened) by an increase in intracellular levels of cyclic AMP. Cyclic AMP opens Cl^- channels by activating cAMP-dependent protein kinase which is thought to phosphorylate either the Cl^- channel itself or an associated regulatory protein. As a result, the rate of transepithelial Cl^- secretion increases. In CF airway epithelia, Cl^- channels are present in the membrane but they cannot be activated by cAMP or cAMP-dependent protein kinase[6,7]. As a result, CF epithelia fail to secrete Cl^- (and thereby fluid) towards the airway lumen. Defective Cl^- secretion probably contributes to the abnormal mucocilliary clearance and lung disease that is the main cause of morbidity and mortality in patients with CF.

The CFTR gene sequence was recently identified and shown to be mutated in patients with CF[8–10]. A 3-base-pair deletion resulting in the loss of a phenylalanine residue at position 508 (ΔF508) occurs in ~70% of CF chromosomes[10,11]. In the accompanying manuscript[12] we describe construction of a full-length CFTR coding sequence. By *in vitro* and *in vivo* synthesis we have shown that CFTR associates with membranes, is a glycoprotein and can be phosphorylated; these properties are consistent with those predicted from the DNA sequence[9]. This work enabled us to test the hypothesis that expression of normal CFTR will complement the CF phenotype and should eventually allow an assessment of the function of CFTR.

Expression of CFTR in CF cells

In evaluating expression systems, we had two main considerations: the protein product should be processed appropriately and most of the cells should express the protein. We chose the vaccinia-T7 hybrid expression system developed by Moss and co-workers[13,14] because it has several advantages, including: (1) infection and expression occur in a wide variety of eukaryotic cells; (2) the virus provides the enzymes necessary for transcription in the cytoplasm of the infected cell, thereby elimininating the need for nuclear processing; (3) the gene product can be correctly processed and targeted to the cell surface; and (4) a high percentage of cells express the recombinant DNA. We were also encouraged to adopt this system because it has been successfully used to express a functional K^+ channel in several cell types[15], including epithelial cells (J.D.McC. and M.J.W., unpublished observations).

In the accompanying manuscript[12] we showed that HeLa cells produced CFTR when they were infected with a recombinant vaccinia virus expressing bacteriophage T7 RNA polymerase, and subsequently transfected with a plasmid containing the T7 promoter and terminator sequences flanking the CFTR coding sequence. We transfected a CF airway epithelial cell line (JME/CF15)[16] with constructs containing either the normal CFTR coding sequence (pTM-CFTR-3), or the mutated CFTR coding sequence (pTM-CFTR-3ΔF508). Figure 1*a* shows expression of CFTR in JME/CF15 cells at 6.5 hours after

§ To whom correspondence should be addressed.

component (τ = 4.7 ns). This τ value is consistent with previous (room temperature) estimates of donor–acceptor center to center distance of 25 Å. The most important result is that the simplified kinetics at room temperature argue that any structural states of the complex which are trapped at 77 K are largely equilibrated at 300 K within 5 ns. This result suggests that motion at the cytc/ccp interface can be quite rapid and offers experimental support for the rapid restricted dimensional diffusion model of the cytc–ccp complex suggested by Brownian dynamics.[8] With this information now available, more detailed insight into the nature of the binding sites in principle could be obtained by comparing the decay distributions for the native systems with those for site-specific mutants.[9,10] Such studies are in progress.

Acknowledgment. We gratefully acknowledge Mark Prichard for assistance with the SPC system. This work was supported by the NIH grant GM-33881 and the SPC system was purchased by the DOE grant DE-FG05-86ER75299. We gratefully acknowledge the ongoing help and interest of Dr. Brian Hoffman and his co-workers.

Characterization of the Soluble All-Carbon Molecules C_{60} and C_{70}

Henry Ajie,[†] Marcos M. Alvarez,[†] Samir J. Anz,[†] Rainer D. Beck,[†] François Diederich,[†] K. Fostiropoulos,[‡] Donald R. Huffman,[§] Wolfgang Krätschmer,[‡] Yves Rubin,[†] Kenneth E. Schriver,[†] Dilip Sensharma,[†] and Robert L. Whetten*,[†]

Department of Chemistry and Biochemistry, University of California, Los Angeles, California 90024-1569; Max-Planck-Institut für Kernphysik, 6900 Heidelberg, Box 103980, F.R.G.; and Department of Physics, University of Arizona, Tucson, Arizona 85721 *(Received: October 3, 1990)*

We report on the further physical and chemical characterization of the new forms of molecular carbon, C_{60} and C_{70}. Our results demonstrate a high yield of production (14%) under optimized conditions and reveal only C_{60} and C_{70} in measurable quantity, in an 85:15 ratio. These two new molecular forms of carbon can be completely separated in analytical amounts by column chromatography on alumina. Comparison among mass spectra obtained by the electron impact, laser desorption, and fast atom bombardment (FAB) methods allows a clear assessment of the composition of the mixed and pure samples, and of the fragmentation and double ionization patterns of the molecules. In addition, spectroscopic analyses are reported for the crude mixture by ^{13}C NMR and by IR spectroscopy in KBr pellet, and for pure C_{60} and C_{70} in solution by UV–vis spectroscopy.

Introduction

In a surprising recent development, Krätschmer et al.[1] have shown that certain all-carbon molecules are produced in large quantities in the evaporation of graphite and can be isolated as soluble, well-defined solids. The major species was identified as molecular C_{60} through mass spectrometry and by comparison of the infrared spectrum with theoretical predictions for the celebrated truncated-icosahedron structure, which had earlier been proposed to account for cluster beam observations.[2] The solid material, described as a new form of elemental carbon in a nearly pure state, has a disordered *hcp* lattice of packed quasi-spherical molecules, but determination of the precise molecular structure awaits diffraction from well-ordered crystals.

Kroto et al.[3] have followed this announcement with a partial chemical separation of the soluble all-carbon molecules generated by the same procedure. They used mass spectrometric evidence to conclude that other air-stable C_n molecules are present (n = 62, 64, 66, 68, 70). They reported that chromatographic separation yields C_{60} and C_{70} in a 3:1 ratio, in contrast to the 2–10% of C_{70} estimated in ref 1. The reported ^{13}C NMR spectrum of the C_{60} fraction, in particular, evidently confirms the existence of a species with all 60 carbon atoms chemically equivalent (proposed structures as shown in Chart I).

This paper describes the further physical and chemical characterization of these two new forms of molecular carbon.[4] Our results include the high-yield production (14%) of soluble material under optimized conditions, consisting of only C_{60} and C_{70} in measurable quantity. These have been separated in analytical amounts by column chromatography and have been characterized in pure or mixed forms by a combination of electron impact, fast atom bombardment (FAB), and laser desorption mass spectrometry. Spectroscopic characterization is reported including the ^{13}C NMR spectrum and the infrared absorption spectrum for the crude C_{60}/C_{70} mixture, and the UV–vis spectrum of pure C_{60} and C_{70} in solution. All five peaks of C_{70} in the ^{13}C NMR spectrum are

CHART I

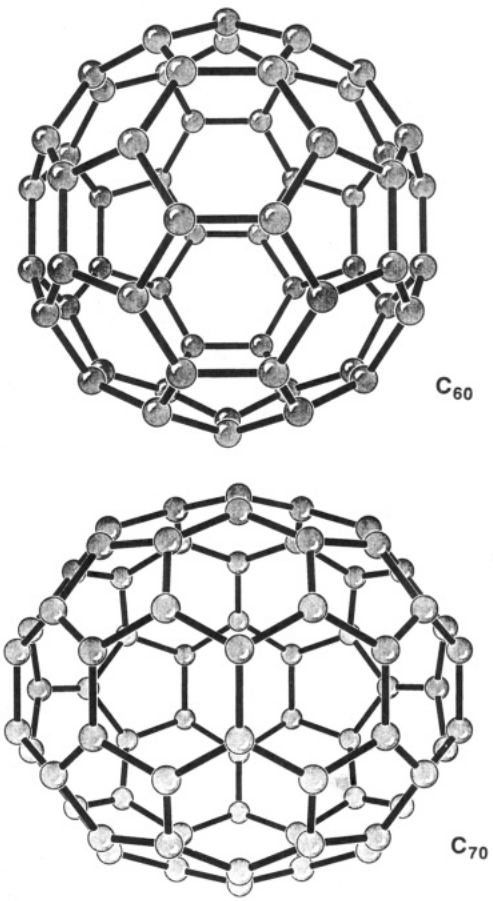

[†] University of California, Los Angeles.
[‡] Max-Planck-Institut für Kernphysik.
[§] University of Arizona.

0022-3654/90/2094-8630$02.50/0

unambiguously found.

Preparation Method and Chromatographic Separation

Two sets of samples have been used in the experiments described below, i.e., one prepared in Heidelberg,[1] used in the earlier stage of this work, and samples newly collected in Los Angeles. We now describe in more detail the method used and yields obtained in the latter preparations. The samples have been prepared following closely the method described by Krätschmer et al.[1] A carbon rod is evaporated by resistive heating under partial helium atmosphere (0.3 bar). The best results were obtained from high-uniformity graphite rods (Poco Graphite, Inc., Type DFP-2, <4 μm grain size, 0.8 μm average pore size). The rods are 1/8 in. diameter and emit a faint gray-white plume when heated by a current of 140–180 A. The sootlike material, collected from the partial evaporation of rods onto a glass shield surrounding the electrodes, is extracted with boiling benzene or toluene to give, after filtration, a brown-red solution. Evaporation yields a brown-black crystalline material in 14% yield (30 mg, identified below to be C_{60} and C_{70}). This yield is higher than reported earlier (ca. 1%,[1b] or "up to 8 percent"[3]) and is believed to be related to the graphite quality and the higher He pressure used. Further evaluation of these methods and yields will follow in a subsequent paper. Chromatographic filtration of the concentrated solution of "crude" material on silica gel with benzene can be performed, but the material obtained remains identical, in all aspects (same C_{60}/C_{70} ratio, no other constituents), to the crude material obtained from the benzene extractions.

Separation of the mixture of C_{60}/C_{70} proved to be a challenging task, particularly because of the poor solubility of the material in most organic solvents. While the solubility in benzene is about 5 mg/mL at 25 °C, the compound is soluble with difficulty at the same temperature in chloroform, dichloromethane, tetrachloromethane, diethyl ether, tetrahydrofuran, *n*-hexane, *n*-pentane, and *n*-octane. The mixture of C_{60}/C_{70} dissolves appreciably better in boiling cyclohexane, from which small black cubes crystallize out on cooling. The material did not melt below 360 °C in a sealed tube; the resulting sample redissolves in benzene, showing no sign of decomposition.

Analytical thin-layer chromatography on silica gel indicated some separation with *n*-hexane or with *n*-pentane as eluents, but not with cyclohexane. Analytical HPLC performed with hexanes (5-μm Econosphere silica, Alltech/Applied Science) gave a satisfactory separation (retention times 6.64 and 6.93 min for C_{60} and C_{70}, respectively, at a flow rate of 0.5 mL/min; detector wavelength, 256 nm), indicating the content of C_{70} to be approximately 15% for the Los Angeles samples. Two other minor peaks, possibly other unidentified C_n species, were observed (retention times 5.86 and 8.31 min), but they constituted less than 1.5% of the total mass.

Column chromatography with hexanes on flash silica gel gave a few fractions of C_{60} with ≥95% purity, as determined by HPLC, along with later fractions containing mixtures of C_{60}/C_{70} in various ratios. Because of the poor solubility of C_{60} and C_{70} in these alkanes, only limited amounts of pure C_{60} were made available this way, in insufficient quantity for a reliable ^{13}C NMR spectrum to be measured (see below). However, column chromatography on neutral alumina with hexanes gave an *excellent* separation in analytical quantities. Thus, pure fractions containing C_{60} (99.85%) and C_{70} (>99%) were obtained, as indicated by mass spectrometric measurements described below.

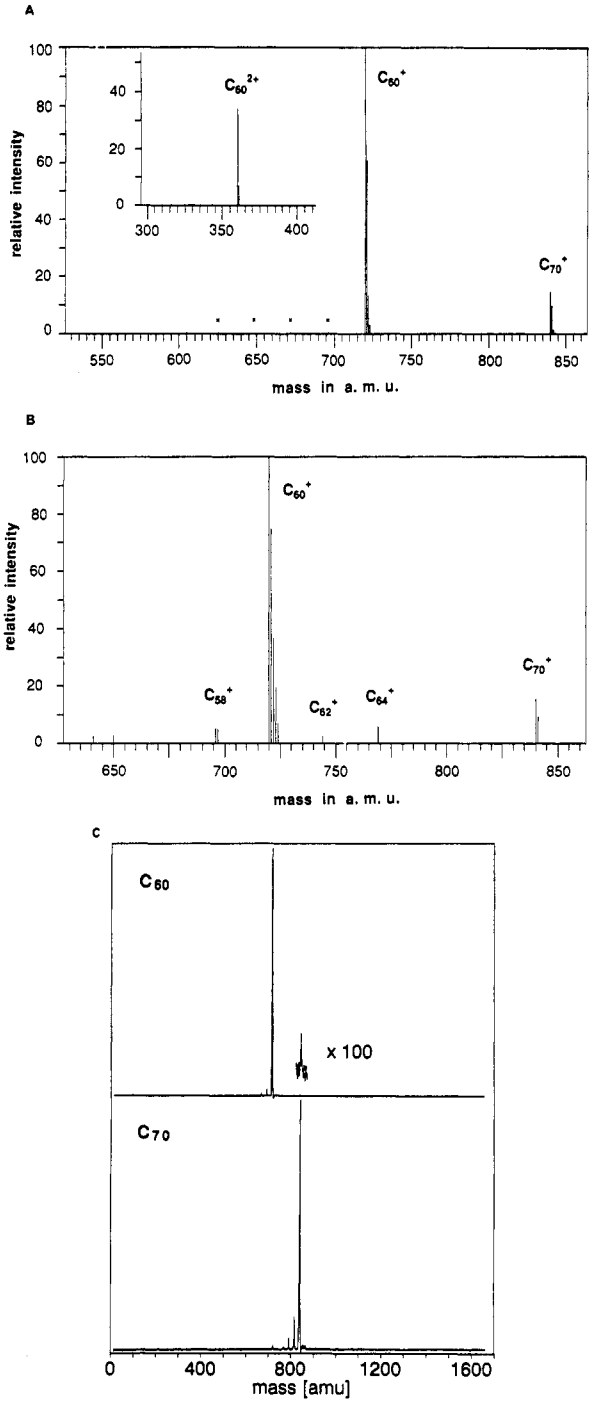

Figure 1. (A) EI MS spectrum of the C_{60} and C_{70} mixture at 70 eV, with a source temperature of 340 °C. Peaks marked with an × are for the ions of C_{58}, C_{56}, C_{54}, and C_{52} at m/z = 696, 672, 648, and 624, respectively. The insert shows the C_{60}^{2+} ion of the same sample. The C_{70}^{2+} ion which also appears in the spectrum is not shown. (B) FAB MS spectrum of the C_{60} and C_{70} mixture with NOBA as the matrix. (C) Laser desorption mass spectra of *pure* C_{60} (above) and C_{70} (below).

Mass Spectrometric Characterization

The 70-eV EI mass spectrometric measurements of the C_{60}/C_{70} mixture's vapor at a source/probe temperature of 340 °C gave exceptionally clean spectra for the samples (Figure 1A). The C_{60}^{+} ion at m/z = 720 and the C_{70}^{+} ion (m/z = 840) are dominant, each with precisely the expected isotopic patterns. The next larger peaks are the doubly charged species C_{60}^{2+} and C_{70}^{2+}, at about one-third of the base-peak intensities, indicating that they must be very stable species as well. At lower ionization energy (16 eV), the doubly charged peaks disappear. From several EI spectra, the average ratio of C_{60} to C_{70} was determined to be 87:13, in striking accordance with the HPLC and the ^{13}C NMR esti-

(1) (a) Krätschmer, W.; Lamb, L. D.; Fostiropoulos, K.; Huffman, D. R. *Nature* **1990**, *347*, 354. (b) Krätschmer, W.; Fostiropoulos, K.; Huffman, D. R. *Chem. Phys. Lett.* **1990**, *170*, 167.

(2) (a) Kroto, H. W.; Heath, J. R.; O'Brien, S. C.; Curl, R. F.; Smalley, R. E. *Nature* **1985**, *318*, 162. (b) Curl, R. F.; Smalley, R. E. *Science* **1988**, *242*, 1017.

(3) Private communication from H. W. Kroto.

(4) D. Bethune et al. have also reported a partial separation by sublimation and Raman spectra of C_{60} and C_{70}; Bethune, D. S.; Meijer, G.; Tang, W. C.; Rosen, H. J. *Chem. Phys. Lett.*, in press.

mations (see below). It seems possible that previous estimates[1a] of the C_{70} content (~2%) of the crude C_{60} samples might have resulted from selective sublimation during the preparation of samples for IR and mass spectrometry. To examine this possibility, we have recorded the apparent abundances of the two molecules as the source/probe temperature is increased from 240 to 340 °C and find that the composition of the vapor changes from >99% C_{60} to the above ratio between 260 and 320 °C. A full analysis of the sublimation properties of these species will be reported separately.

The 70-eV EI spectrum of Figure 1A also contains peaks of C_{58}, C_{56}, C_{54}, and C_{52} at m/z = 696, 672, 648, and 624, respectively, corresponding to the expected fragmentation pattern.[5] Because they fail to appear at 16 eV, they must presumably result from fragmentation of the C_{60}^+ ion, yet their low abundance (0.8% summed together) suggests a very high stability to the carbon cage of C_{60}.

The fast atom bombardment (FAB) mass spectra of the *same* material were again astonishingly simple (Figure 1B), revealing only C_{58}, C_{62}, and C_{64} species besides the C_{60}^+ and the C_{70}^+ ions. No peaks were found beyond m/z = 840/841/842 (up to m/z = 1200), thus indicating the absence of higher mass C_n species. In agreement with the EI spectra of the high-temperature vapor, the FAB results indicated the C_{60}/C_{70} ratio to be 87:13. However, the minority species are more abundant than in the EI spectra and are probably the result of intermolecular reactions/fragmentations in the *m*-nitrobenzyl alcohol (NOBA) matrix used in FAB MS.

The laser desorption method is less destructive than the FAB method, but shares the feature of not requiring a continuous, long-time heating of the sample.[6b] Accordingly, the very clean LD mass spectra of C_{60} and C_{70} (Figure 1C) were obtained by time-of-flight analysis of the ions desorbed when 266-nm laser pulses were directed into a pulsed He jet flowing over the sample. On the crude mixture of C_{60}/C_{70}, it was found that all features of (0–2000 amu) except C_{60} and C_{70} vanished at the lowest laser fluences, and these exhibited the same ratio (88:12), within experimental uncertainty, as found in the high-temperature EI mass spectra. When applied to the samples of C_{60} and C_{70} separated by column chromatography on alumina, the C_{60} fraction was found to have a purity of 99.85%, with C_{70} as the residual. On the other hand, the C_{70} fraction had a purity of >99%; the minor peaks, corresponding to C_{68}, C_{66}, C_{64}, and C_{60}, are found by careful analysis of the laser-fluence dependence to all be fragmentation products of C_{70}. In particular, the relative intensity of the C_{60} peak increased directly with increasing laser fluence, thus demonstrating that it results from the fragmentation of C_{70}.

Carbon-13 NMR Spectra

The crude samples of C_{60}/C_{70} obtained from our two sources were independently investigated by ^{13}C NMR and gave identical results. Since it was expected that the spin–lattice relaxation time of the ^{13}C nuclei would be quite long, an inversion recovery experiment was performed to obtain a rough estimate of T_1. Thus, it was determined that T_1 for C_{60} was ≥20 s. The samples of C_{60}/C_{70} were dissolved in an excess of benzene-d_6 and evaporated at 25 °C until saturation was achieved. Using a 30-deg pulse and a 20-s pulse delay, a total of 5780 accumulations obtained over 32 h on a Bruker AM 360 instrument (90.56 MHz) gave a spectrum with an acceptable signal/noise ratio, showing clearly the presence of C_{60} and C_{70} only (Figure 2B). Thus, the peak corresponding to C_{60} is observed at 143.2 ppm (cf. ref 3), and the peaks at 130.9, 145.4, 147.4, 148.1, and 150.7 ppm are attributed to C_{70}, the number of carbons and the 10/20/10/20/10 peak ratio being as expected for the proposed molecular structure.

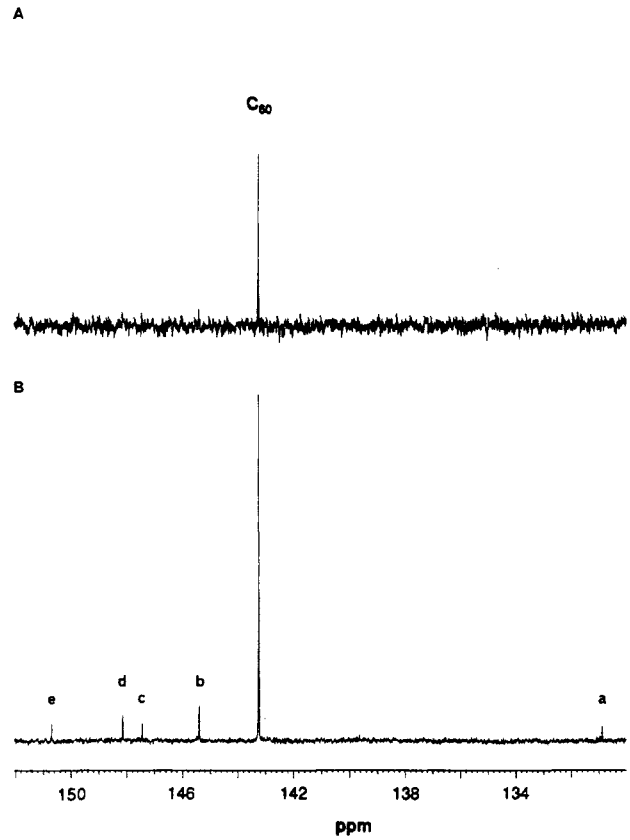

Figure 2. (A) ^{13}C NMR spectrum of a C_{60} and C_{70} mixture in benzene-d_6 at 296 K after 484 accumulations with a 2-s delay between 30-deg pulses. (B) Same sample after 5780 accumulations with a 20-s delay between pulses. Peaks labeled a, b, c, d, and e are assigned to C_{70}. Both spectra are plotted from 130 to 152 ppm.

The ^{13}C NMR spectrum shown in Figure 2A was performed on the same sample with only 484 accumulations with a 2-s delay between pulses. Thus it is possible to see the single C_{60} peak in a very short time during the experiment. This demonstrates that erroneous interpretations about the purity of the sample can be made if too few accumulations or a less sensitive instrument is used.

With relaxation times for the ^{13}C nuclei of C_{60} and C_{70} being probably very similar, an estimate of the ratio of the two compounds (Figure 2B) by comparison of the peak heights was expected to give a good estimate of the composition of the compound. Thus, the ratio was determined to be 82:18, in reasonable accordance with the HPLC and mass spectrometric determinations described above.

As expected, the proton NMR spectra of the samples dissolved in benzene-d_6 were devoid of any absorptions besides the C_6D_5H peak at 7.15 ppm and a few impurities at 0.3–1.4 ppm, also present in neat solvent.

Optical Absorption Spectra

In ref 1, the optical absorption spectrum in the ultraviolet and visible region was reported for the sublimed C_{60}/C_{70} mixture as a neat solid film. In our work, the spectra of pure C_{60} and C_{70} were recorded in *n*-hexane. Figure 3 shows the absorption spectra in the 200–800-nm region for C_{60} (99.85% purity) and C_{70} (>99%) at 25 °C. Compared with the spectrum of ref 1, one observes small hypsochromic shifts of the peak maxima of C_{60} and alterations in relative intensities as a result of removing the C_{70} contaminant. In addition, the spectrum of pure C_{70} appears to be distinct from any previously reported, including the brief list of maxima given for a sample of unstated purity in ref 3.

Absorption by C_{60} begins with an abrupt onset of 635 nm, followed by several bands of varying width (centered at 621, 598, 591, 568, 540, and 492 nm), and a highly transparent region at 420–440 nm. The structure of the visible absorption spectrum

(5) Radi, P. P.; Bunn, T. L.; Kemper, P. R.; Molchan, M. E.; Bowers, M. T. *J. Chem. Phys.* **1988**, *88*, 2809.

(6) (a) For the gas-phase synthesis of another carbon allotrope, C_{18}, see: Diederich, F.; Rubin, Y.; Knobler, C. B.; Whetten, R. L.; Schriver, K. E.; Houk, K. N.; Li, Y. *Science* **1989**, *245*, 1088. (b) For a preparation of C_{60} and C_{70} starting from molecular precursors, see: Rubin, Y.; Kahr, M.; Knobler, C. B.; Diederich, F.; Wilkins, C. L. *J. Am. Chem. Soc.*, in press.

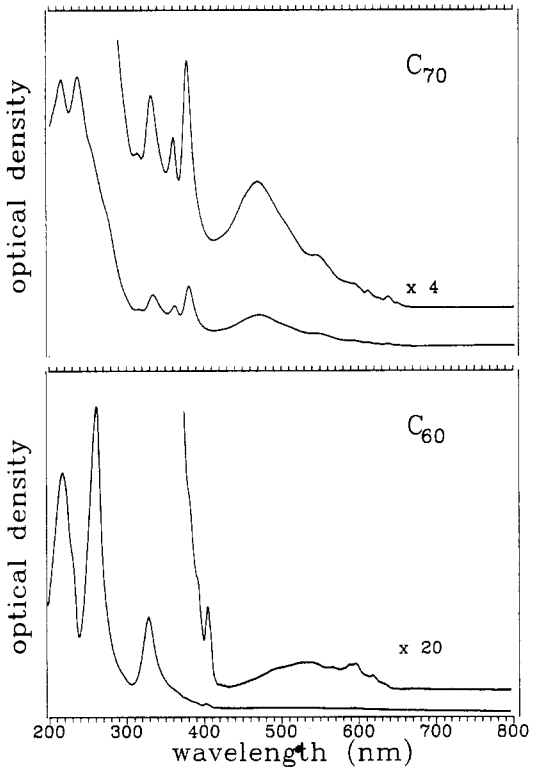

Figure 3. (A, top) Electronic absorption spectrum of dilute C_{70} in hexanes at 25 °C. The insert is the spectrum of the same sample at 4× concentration. (B, bottom) Electronic absorption spectrum of dilute C_{60} in hexanes at 25 °C. The insert is the spectrum of the same sample at 20× concentration.

is suggestive of vibrational structure from one or two forbidden electronic transitions. The combination of transparency in this blue region and in the red (>635 nm) gives dilute solutions a distinct purple color to the eye. A second onset leading to stronger absorption occurs in the form of a band at 404 nm, with a shoulder at 408 nm. These are followed by distinct shoulders at 396, 391, 377, and 365 nm, also suggestive of vibrational structure, appearing on a strong rise toward the first major maximum at 328 nm. The ultraviolet region is dominated by this feature and two other strong broad bands peaking at 211 and 256 nm, the former with a shoulder at 227 nm.

Based on these results, it seems unlikely that neutral C_{60} is the carrier of the interstellar 220-nm absorption band,[7] as the 255- and 330-nm peaks are not concurrently observed.

Absorption by C_{70} begins with a weak onset band at 650 nm, followed by a series of peaks (637, 624, 610, 600, and 594 nm) superimposed on a gradually rising continuum leading to stronger maxima at 544 and 469 nm. A broad minimum covers the blue-violet region, and maxima of intermediate strength appear in the near-ultraviolet region at 378, 359, and 331 nm. Following a weaker maximum at 313 nm, very strong absorptions appear with three shoulders leading to the dominant bands at 236 and 215 nm. Dilute C_{70} solutions are orange-red in color. Detailed comparison of the spectra indicates no coincidences between C_{70} and C_{60} bands, as would be expected from the purities stated above.

The FT-IR spectrum of the C_{60} and C_{70} mixture performed with a conventional KBr pellet showed the four strongest bands for C_{60} at 1430, 1182, 577, and 527 cm^{-1}, as observed previously by Krätschmer et al.[1] In addition, the strong peak at 673 cm^{-1} mentioned by these authors was present, together with a smaller peak at 795 cm^{-1}.

Conclusion

The new molecular forms of carbon, C_{60} and C_{70}, were prepared following the method of Krätschmer et al.[1] in a consistently high yield (14%).[1] The benzene-soluble material extracted from the graphite evaporation product is predominantly constituted of C_{60} and C_{70}. Three independent methods, namely HPLC, mass spectroscopy, and ^{13}C NMR, demonstrate that these two compounds are present in a ratio near 85:15. The two compounds can be separated by column chromatography on alumina, allowing as for now the purification of minute quantities of pure C_{60} and C_{70}. Support for the proposed symmetrical cage structures (fullerenes) of C_{60} and C_{70} is inferred from the simplicity of the ^{13}C NMR spectra and the strong presence of the C_{60}^{2+} and C_{70}^{2+} ions. Attempts at the X-ray determination of the C_{60} molecular structure are now actively pursued.[6]

Note Added in Proof. The soluble byproduct (HPLC retention time 8.31 min) has since been isolated and determined to be C_{84} by laser desorption MS. The ^{13}C NMR spectrum of *pure* C_{70} (in 1,1,2,2-tetrachloroethane-d_2) has *only* the five lines at 131.0, 145.4, 147.5, 148.2, and 150.8 ppm.

Acknowledgment. We thank Prof. B. Dunn and his students for their generous help with the carbon evaporator, C. B. Knobler for several attempts at the diffractometer and for discussions about the crystallization of the compound, J. M. Strouse for her assistance in the ^{13}C NMR experiments, and H. W. Kroto and D. Bethune for communication of unpublished results. The work in Los Angeles was supported by the National Science Foundation and by Office of Naval Research contracts to RLW and FND.

(7) Huffman, D. R. *Adv. Phys.* **1977**, *26*, 129.